

ISSN(ONLINE):2045-8711
ISSN(PRINT) :2045-869X



International Journal
of Innovative Technology
& Creative Engineering

July 2012
Vol.2 No.7

©IJITCE PUBLICATION

UK: Managing Editor

International Journal of Innovative Technology and Creative Engineering
1a park lane,
Cranford
London
TW59WA
UK
E-Mail: editor@ijitce.co.uk
Phone: +44-773-043-0249

USA: Editor

International Journal of Innovative Technology and Creative Engineering
Dr. Arumugam
Department of Chemistry
University of Georgia
GA-30602, USA.
Phone: 001-706-206-0812
Fax:001-706-542-2626

India: Editor

International Journal of Innovative Technology & Creative Engineering
Dr. Arthanarisee. A. M
Finance Tracking Center India
17/14 Ganapathy Nagar
2nd Street
Ekkattuthangal
Chennai -600032
Mobile: 91-7598208700

www.ijitce.co.uk

IJITCE PUBLICATION

**INTERNATIONAL JOURNAL OF INNOVATIVE
TECHNOLOGY & CREATIVE ENGINEERING**

Vol.2 No.7

July 2012

www.ijitce.co.uk

From Editor's Desk

Dear Researcher,

Greetings!

Research article in this issue discusses about

Let us review research around the world this month; A recently launched Web site, LabSafetyWorkspace.org, offers free, short safety training courses to scientists everywhere. It is a joint project of the New Hampshire IDeA Network of Biological Research Excellence (NH-INBRE), a consortium of 10 New Hampshire colleges and universities that is funded by the National Institutes of Health. The site is primarily aimed at students and the courses are open to scientists at any stage and any age who wish to use its materials. The courses range in length from about 20 minutes to 2 hours.

European non-profit researchers' association Euroscience launched a survey exploring the working conditions and career development of young researchers. The aim: to fill in gaps in comparable data across European countries to better identify the career needs of young researchers and help improve their situations. So far, about 1900 Masters' students, Ph.D candidates, postdocs, and industry employees have taken part.

Results from two experiments at the Large Hadron Collider in Europe confirmed the existence of a new heavy particle, likely to be the long-sought Higgs boson, thanks to troves of particle-collision data that yielded discovery-level certainty upon analysis. The results, announced at a major particle physics conference in Melbourne, Australia, mark the culmination of a search for a heavy particle believed to give mass to elementary particles such as electrons and quarks.

While in a recession, New York City has managed to increase tech related jobs by 28.7% from 41,100 to 52,900 and added 486 digital startups formed since 2007. While New York has not seen such high percentages of unemployment since The Great Depression, it continues to be amazing that people are still managing to open up their own businesses.

It has been an absolute pleasure to present you articles that you wish to read. We look forward to many more new technology-related research articles from you and your friends. We are anxiously awaiting the rich and thorough research papers that have been prepared by our authors for the next issue.

Thanks,
Editorial Team
IJITCE

Editorial Members

Dr. Chee Kyun Ng Ph.D

Department of Computer and Communication Systems,
Faculty of Engineering, Universiti Putra Malaysia, UPM Serdang, 43400 Selangor, Malaysia.

Dr. Simon SEE Ph.D

Chief Technologist and Technical Director at Oracle Corporation, Associate Professor (Adjunct) at Nanyang Technological University
Professor (Adjunct) at Shanghai Jiaotong University, 27 West Coast Rise #08-12, Singapore 127470

Dr. sc.agr. Horst Juergen SCHWARTZ Ph.D,

Humboldt-University of Berlin, Faculty of Agriculture and Horticulture, Astenplatz 2a, D-12203 Berlin, Germany

Dr. Marco L. Bianchini Ph.D

Italian National Research Council; IBAF-CNR, Via Salaria km 29.300, 00015 Monterotondo Scalo (RM), Italy

Dr. Nijad Kabbara Ph.D

Marine Research Centre / Remote Sensing Centre/ National Council for Scientific Research,
P. O. Box: 189 Jounieh, Lebanon

Dr. Aaron Solomon Ph.D

Department of Computer Science,
National Chi Nan University, No. 303, University Road, Puli Town, Nantou County 54561, Taiwan

Dr. Arthanariee. A. M M.Sc., M.Phil., M.S., Ph.D

Director - Bharathidasan School of Computer Applications, Ellispettai, Erode, Tamil Nadu, India

Dr. Takaharu KAMEOKA, Ph.D

Professor, Laboratory of Food,
Environmental & Cultural Informatics Division of Sustainable Resource Sciences,
Graduate School of Bioresources, Mie University, 1577 Kurimamachiya-cho, Tsu, Mie, 514-8507, Japan

Mr. M. Sivakumar M.C.A., ITIL., PRINCE2., ISTQB., OCP., ICP

Project Manager - Software, Applied Materials, 1a park lane, cranford, UK

Dr. Bulent Acma Ph.D

Anadolu University,
Department of Economics, Unit of Southeastern Anatolia Project(GAP), 26470 Eskisehir, TURKEY

Dr. Selvanathan Arumugam Ph.D

Research Scientist, Department of Chemistry, University of Georgia, GA-30602, USA.

Review Board Members

Dr. Paul Koltun

Senior Research Scientist LCA and Industrial Ecology Group, Metallic & Ceramic Materials, CSIRO Process Science & Engineering Private Bag 33, Clayton South MDC 3169, Gate 5 Normanby Rd., Clayton Vic. 3168, Australia

Dr. Zhiming Yang MD., Ph. D.

Department of Radiation Oncology and Molecular Radiation Science, 1550 Orleans Street Rm 441, Baltimore MD, 21231, USA

Dr. Jifeng Wang

Department of Mechanical Science and Engineering, University of Illinois at Urbana-Champaign Urbana, Illinois, 61801, USA

Dr. Giuseppe Baldacchini

ENEA - Frascati Research Center, Via Enrico Fermi 45 - P.O. Box 65, 00044 Frascati, Roma, ITALY.

Dr. Mutamed Turki Nayef Khatib

Assistant Professor of Telecommunication Engineering, Head of Telecommunication Engineering Department, Palestine Technical University (Kadoorie), Tul Karm, PALESTINE.

Dr.P.Uma Maheswari

Prof & Head, Department of CSE/IT, INFO Institute of Engineering, Coimbatore.

Dr. T. Christopher, Ph.D.,

Assistant Professor & Head, Department of Computer Science, Government Arts College (Autonomous), Udumalpet, India.

Dr. T. DEVI Ph.D. Engg. (Warwick, UK),

Head, Department of Computer Applications, Bharathiar University, Coimbatore-641 046, India.

Dr. Renato J. Orsato

Professor at FGV-EAESP, Getulio Vargas Foundation, São Paulo Business School, Rua Itapeva, 474 (8º andar), 01332-000, São Paulo (SP), Brazil
Visiting Scholar at INSEAD, INSEAD Social Innovation Centre, Boulevard de Constance, 77305 Fontainebleau - France

Y. Benal Yurtlu

Assist. Prof. Ondokuz Mayıs University

Dr. Sumeer Gul

Assistant Professor, Department of Library and Information Science, University of Kashmir, India

Dr. Chutima Boonthum-Denecke, Ph.D

Department of Computer Science, Science & Technology Bldg., Rm 120, Hampton University, Hampton, VA 23688

Dr. Renato J. Orsato

Professor at FGV-EAESP, Getulio Vargas Foundation, São Paulo Business School, Rua Itapeva, 474 (8º andar), 01332-000, São Paulo (SP), Brazil

Dr. Lucy M. Brown, Ph.D.

Texas State University, 601 University Drive, School of Journalism and Mass Communication, OM330B, San Marcos, TX 78666

Javad Robati

Crop Production Department, University of Maragheh, Golshahr, Maragheh, Iran

Vinesh Sukumar (PhD, MBA)

Product Engineering Segment Manager, Imaging Products, Aptina Imaging Inc.

Dr. Binod Kumar PhD(CS), M.Phil.(CS), MIAENG, MIEEE

HOD & Associate Professor, IT Dept, Medi-Caps Inst. of Science & Tech. (MIST), Indore, India

Dr. S. B. Warkad

Associate Professor, Department of Electrical Engineering, Priyadarshini College of Engineering, Nagpur, India

Dr. doc. Ing. Rostislav Choteborský, Ph.D.

Katedra materiálu a strojírenské technologie Technická fakulta, Česká zemědělská univerzita v Praze, Kamýcká 129, Praha 6, 165 21

Dr. Paul Koltun

Senior Research Scientist LCA and Industrial Ecology Group, Metallic & Ceramic Materials, CSIRO Process Science & Engineering Private Bag 33, Clayton South MDC 3169, Gate 5 Normanby Rd., Clayton Vic. 3168

DR. Chutima Boonthum-Denecke, Ph.D

Department of Computer Science, Science & Technology Bldg., Hampton University, Hampton, VA 23688

Mr. Abhishek Taneja B.sc(Electronics), M.B.E, M.C.A., M.Phil.,

Assistant Professor in the Department of Computer Science & Applications, at Dronacharya Institute of Management and Technology, Kurukshetra. (India).

Dr. Ing. Rostislav Choteborský, ph.d,

Katedra materiálu a strojírenské technologie, Technická fakulta, Česká zemědělská univerzita v Praze, Kamýcká 129, Praha 6, 165 21

Dr. Amala VijayaSelvi Rajan, B.sc,Ph.d,

Faculty – Information Technology Dubai Women’s College – Higher Colleges of Technology,P.O. Box – 16062, Dubai, UAE

Naik Nitin Ashokrao B.sc,M.Sc

Lecturer in Yeshwant Mahavidyalaya Nanded University

Dr.A.Kathirvell, B.E, M.E, Ph.D,MISTE, MIACSIT, MENG

Professor - Department of Computer Science and Engineering,Tagore Engineering College, Chennai

Dr. H. S. Fadewar B.sc,M.sc,M.Phil.,ph.d,PGDBM,B.Ed.

Associate Professor - Sinhgad Institute of Management & Computer Application, Mumbai-Banglore Westernly Express Way Narhe, Pune - 41

Dr. David Batten

Leader, Algal Pre-Feasibility Study,Transport Technologies and Sustainable Fuels,CSIRO Energy Transformed Flagship Private Bag 1,Aspendale, Vic. 3195,AUSTRALIA

Dr R C Panda

(MTech & PhD(IITM);Ex-Faculty (Curtin Univ Tech, Perth, Australia))Scientist CLRI (CSIR), Adyar, Chennai - 600 020,India

Miss Jing He

PH.D. Candidate of Georgia State University,1450 Willow Lake Dr. NE,Atlanta, GA, 30329

Jeremiah Neubert

Assistant Professor,Mechanical Engineering,University of North Dakota

Hui Shen

Mechanical Engineering Dept,Ohio Northern Univ.

Dr. Xiangfa Wu, Ph.D.

Assistant Professor / Mechanical Engineering,NORTH DAKOTA STATE UNIVERSITY

Seraphin Chally Abou

Professor,Mechanical & Industrial Engineering Depart,MEHS Program, 235 Voss-Kovach Hall,1305 Ordean Court,Duluth, Minnesota 55812-3042

Dr. Qiang Cheng, Ph.D.

Assistant Professor,Computer Science Department Southern Illinois University CarbondaleFaner Hall, Room 2140-Mail Code 45111000 Faner Drive, Carbondale, IL 62901

Dr. Carlos Barrios, PhD

Assistant Professor of Architecture,School of Architecture and Planning,The Catholic University of America

Y. Benal Yurtlu

Assist. Prof. Ondokuz Mayis University

Dr. Lucy M. Brown, Ph.D.

Texas State University,601 University Drive,School of Journalism and Mass Communication,OM330B,San Marcos, TX 78666

Dr. Paul Koltun

Senior Research ScientistLCA and Industrial Ecology Group,Metallic & Ceramic Materials CSIRO Process Science & Engineering

Dr.Sumeer Gul

Assistant Professor,Department of Library and Information Science,University of Kashmir,India

Dr. Chutima Boonthum-Denecke, Ph.D

Department of Computer Science,Science & Technology Bldg., Rm 120,Hampton University,Hampton, VA 23688

Dr. Renato J. Orsato

Professor at FGV-EAESP,Getulio Vargas Foundation,São Paulo Business School,Rua Itapeva, 474 (8° andar) 01332-000, São Paulo (SP), Brazil

Dr. Wael M. G. Ibrahim

Department Head-Electronics Engineering Technology Dept.School of Engineering Technology ECPI College of Technology 5501 Greenwich Road - Suite 100,Virginia Beach, VA 23462

Dr. Messaoud Jake Bahoura

Associate Professor-Engineering Department and Center for Materials Research Norfolk State University,700 Park avenue,Norfolk, VA 23504

Dr. V. P. Eswaramurthy M.C.A., M.Phil., Ph.D.,

Assistant Professor of Computer Science, Government Arts College(Autonomous), Salem-636 007, India.

Dr. P. Kamakkannan,M.C.A., Ph.D .,

Assistant Professor of Computer Science, Government Arts College(Autonomous), Salem-636 007, India.

Dr. V. Karthikeyani Ph.D.,

Assistant Professor of Computer Science, Government Arts College(Autonomous), Salem-636 008, India.

Dr. K. Thangadurai Ph.D.,

Assistant Professor, Department of Computer Science, Government Arts College (Autonomous), Karur - 639 005,India.

Dr. N. Maheswari Ph.D.,

Assistant Professor, Department of MCA, Faculty of Engineering and Technology, SRM University, Kattangulathur, Kanchipiram Dt - 603 203, India.

Mr. Md. Musfique Anwar B.Sc(Engg.)

Lecturer, Computer Science & Engineering Department, Jahangirnagar University, Savar, Dhaka, Bangladesh.

Mrs. Smitha Ramachandran M.Sc(CS),

SAP Analyst, Akzonobel, Slough, United Kingdom.

Dr. V. Vallimayil Ph.D.,

Director, Department of MCA, Vivekanandha Business School For Women, Elayampalayam, Tiruchengode - 637 205, India.

Mr. M. Moorthi M.C.A., M.Phil.,

Assistant Professor, Department of computer Applications, Kongu Arts and Science College, India

Prema Selvaraj Bsc,M.C.A,M.Phil

Assistant Professor,Department of Computer Science,KSR College of Arts and Science, Tiruchengode

Mr. G. Rajendran M.C.A., M.Phil., N.E.T., PGDBM., PGDBF.,

Assistant Professor, Department of Computer Science, Government Arts College, Salem, India.

Dr. Pradeep H Pendse B.E.,M.M.S.,Ph.d

Dean - IT,Welingkar Institute of Management Development and Research, Mumbai, India

Muhammad Javed

Centre for Next Generation Localisation, School of Computing, Dublin City University, Dublin 9, Ireland

Dr. G. GOBI

Assistant Professor-Department of Physics,Government Arts College,Salem - 636 007

Dr.S.Senthilkumar

Post Doctoral Research Fellow, (Mathematics and Computer Science & Applications),Universiti Sains Malaysia,School of Mathematical Sciences, Pulau Pinang-11800,[PENANG],MALAYSIA.

Manoj Sharma

Associate Professor Deptt. of ECE, Prannath Parnami Institute of Management & Technology, Hissar, Haryana, India

RAMKUMAR JAGANATHAN

Asst-Professor,Dept of Computer Science, V.L.B Janakiammal college of Arts & Science, Coimbatore,Tamilnadu, India

Dr. S. B. Warkad

Assoc. Professor, Priyadarshini College of Engineering, Nagpur, Maharashtra State, India

Dr. Saurabh Pal

Associate Professor, UNS Institute of Engg. & Tech., VBS Purvanchal University, Jaunpur, India

Manimala

Assistant Professor, Department of Applied Electronics and Instrumentation, St Joseph's College of Engineering & Technology, Choondacherry Post, Kottayam Dt. Kerala -686579

Dr. Qazi S. M. Zia-ul-Haque

Control Engineer Synchrotron-light for Experimental Sciences and Applications in the Middle East (SESAME), P. O. Box 7, Allan 19252, Jordan

Dr. A. Subramani, M.C.A., M.Phil., Ph.D.

Professor, Department of Computer Applications, K.S.R. College of Engineering, Tiruchengode - 637215

Dr. Seraphin Chally Abou

Professor, Mechanical & Industrial Engineering Depart. MEHS Program, 235 Voss-Kovach Hall, 1305 Ordean Court Duluth, Minnesota 55812-3042

Dr. K. Kousalya

Professor, Department of CSE, Kongu Engineering College, Perundurai-638 052

Dr. (Mrs.) R. Uma Rani

Asso.Prof., Department of Computer Science, Sri Sarada College For Women, Salem-16, Tamil Nadu, India.

MOHAMMAD YAZDANI-ASRAMI

Electrical and Computer Engineering Department, Babol "Noshirvani" University of Technology, Iran.

Dr. Kulasekharan, N, Ph.D

Technical Lead - CFD, GE Appliances and Lighting,

GE India, John F Welch Technology Center, Plot # 122, EPIP, Phase 2, Whitefield Road, Bangalore – 560066, India.

Dr. Manjeet Bansal

Dean (Post Graduate), Department of Civil Engineering, Punjab Technical University, Giani Zail Singh Campus, Bathinda -151001 (Punjab), INDIA

Dr. Oliver Juki

Vice Dean for education, Virovitica College, Matije Gupca 78, 33000 Virovitica, Croatia

Dr. Lori A. Wolff, Ph.D., J.D.

Professor of Leadership and Counselor Education, The University of Mississippi, Department of Leadership and Counselor Education, 139 Guyton University, MS 38677

Contents

Convective Heat Transfer in a Vertical Channel Filled with a Nanofluid by J.C. Umavathia, K.V. Prasad and M. Shekara[1]

An Experimental Study of Effect of Welding Parameters on T- Weld Joint in TIG Welding of SS 316L and Development of its Microstructure and Mechanical properties by Rupinderpreet Singh, Geetesh Goga, Lakhwinder Singh[2]

Convective Heat Transfer in a Vertical Channel Filled with a Nanofluid

J.C. Umavathi^a, K.V. Prasad^b and M. Shekar^a

^aDepartment of Mathematics, Gulbarga University, Gulbarga, Karnataka, India

^bDepartment of Mathematics, Central College campus, Bangalore University, Bangalore, Karnataka, India.

^bcorresponding author: prasadvk2000@yahoo.co.in

Abstract— Nanofluids are engineered colloids made of a base fluid and nanoparticles (1-100 nm). This article presents the numerical study of a natural convection flow and heat transfer characteristics in a vertical channel filled with a nanofluid. The transport equations along with the boundary conditions are first cast into a dimensionless form and then the resulting equations are solved numerically by finite difference method. Also, we compared the numerical results using semi-numerical-analytical method known as Differential Transformation Method (DTM), and regular perturbation method (PM). The influence of pertinent parameters such as Grashof number, Brinkman number and the nanoparticle volume fraction on the velocity and temperature fields are shown graphically. Results for the skin friction and heat transfer rate for various types of nanoparticles such as Ag-water, Cu-water, SiO₂-water, Diamond-water and TiO₂-water are also tabulated. The results obtained for the flow and heat transfer characteristics reveal many interesting behaviors that warrant further study on nanofluids in a vertical channel.

Keywords: Natural convection, nanofluid, Differential transformation method, Finite difference method, perturbation method.

I. INTRODUCTION

Natural convection heat transfer has been considered by many designers in the past as an important phenomenon in the cooling mechanism of engineering systems due to its simplicity, minimum cost, low noise, smaller size, and reliability. Ostrach [1] was the first among others to reviewed various industrial and engineering applications of natural convection such as thermal insulators for buildings, the electronics industry, solar collectors, and cooling systems for nuclear reactors. Recently, using

nanofluids as an advanced technology has a tendency to increase the heat transfer compared to other base fluids. This technology lies under the concepts of using suspended nanoparticles in order to enhance the rate of heat transfer.

Enhancement of heat transfer is essential in improving performances and compactness of electronic devices. Usual cooling agents (water, oil, etc.) have relatively small thermal conductivities and therefore heat transfer is not very efficient. Therefore numerous methods were proposed to improve the thermal conductivity of these fluids by suspending nano/micro (larger-size) particle materials in liquids. An innovative technique, which uses a mixture of nanoparticles and the base fluid, was first introduced by Choi [2] in order to develop advanced heat transfer fluids with substantially higher conductivities. The resulting mixture of the base fluid and nanoparticles having unique physical and chemical properties is referred to as a nanofluid. Nanofluid describes a liquid suspension containing ultra-fine particles (diameter less than 50 nm). Experimental studies show that even with small volumetric fraction of nanoparticles (usually less than 5%) the thermal conductivity of the base fluid is enhanced by 10-50% with a remarkable improvement in the convective heat transfer coefficient. The characteristic feature of nanofluid is the thermal conductivity enhancement, a phenomenon observed by Masuda et al. [3]. This suggested the possible use of nanofluids in advanced nuclear systems (Buongiorno and Hu [4]). Eastman et al. [5], Xie et al. [6] and Jana et al. [7] showed that higher thermal conductivity can be achieved in thermal systems utilizing nanofluids. Few researchers considered the fluid and solid phase role in the heat transfer process as two-phase model while the others considered both the fluid phase and the solid particles in a thermal equilibrium state and flow with the same local velocity (single phase). Various literatures have mentioned that the two-phase model is not applicable for analyzing nanofluids [8-9]. Owing to their superior characteristic, nanofluids behave like a fluid rather than an unconventional solid/fluid mixture fluid containing micron and large particles. For this reason the application of the modified single phase method is more appropriate for the heat transfer process. Several investigations have been reported in the literature on the convective heat transfer in nanofluids; see, for example, Daungthongsuk and Wongwises [10],

Trisaksri and Wongwises [11], Wang and Mujumdar [12], Kumar et al. [13] and the references cited therein. Recently Cimpean and Pop [14] studied analytically the fully developed mixed convection flow of a nanofluid through an inclined channel filled with a porous medium.

The differential transformation method (DTM) was first applied in the engineering domain by Zhou [15]. The differential transform method is based on Taylor expansion. It constructs an analytical solution in the form of a polynomial. It is different from the traditional high order Taylor series method, which requires symbolic computation of the necessary derivatives of the data functions. The Taylor series method is computationally taken long time for large orders. The differential transform is an iterative procedure for obtaining analytic Taylor series solutions of differential equations. DTM has been successfully applied to solve many nonlinear problems arising in engineering, physics, mechanics, biology, etc. The differential transform method can overcome the restrictions and limitations of perturbation techniques so that it provides us with a possibility to analyze strongly nonlinear problems. Jang et al. [16] applied the two-dimensional differential transform method to the solution of partial differential equations. Kurnaz and Oturanç [17] applied DTM for solution of system of ordinary differential equations. Arikoglu and Ozkol [18] employed DTM on differential-difference equations. Ravi Kanth and Aruna [19] found the solution of singular two-point boundary value problems using differential transformation method. The method was successfully applied to various application problems [20–24]. Very recently Rashidi et al. [25] applied the DTM to obtain approximate analytical solutions of combined free and forced (mixed) convection about inclined surfaces in a saturated porous medium.

Despite a number of experimental and numerical studies on convection flow in nanofluids (reported in the literature), there is still a lack of information on the problem of heat transfer enhancement in a vertical channel containing water based nanofluids. In fact to the best knowledge of the authors, no studies have been reported in the literature.

The focus of the present study is to analyze the effects of several pertinent parameters such as the free convection parameter, nanoparticle-size volume fraction; and Brinkman number on the flow and heat transfer characteristics with different types of nanofluid particles. The coupled non-linear ordinary differential equations are solved analytically using DTM valid for all values of free convection parameter and Brinkman number. To validate the DTM solutions, the basic equations are solved by numerical method using finite difference method and also analytically using regular perturbation method valid for small values of free convection parameter and Brinkman number.

II. PROBLEM DESCRIPTION AND GOVERNING EQUATIONS

Consider an incompressible water-based nanofluid, which steadily flows between two infinite vertical and parallel plate walls maintained at different constant temperatures extending in the X and Y directions, as shown in Figure 1. The differentially heated walls are filled with a water based nanofluid containing different types of nano-solidparticles namely copper (Cu), silver (Ag), Titanium (TiO_2), silicon (SiO_2) and Diamond. The nano-solidparticles is Newtonian, incompressible, and laminar. The base fluid and the spherical nanoparticles are in thermal equilibrium. The nanofluid is a two component mixture with the following assumptions:

- i. steady, laminar and fully developed;
- ii. incompressible;
- iii. no-chemical reaction;
- iv. negligible radiative heat transfer; and
- v. nano-solid-particles and the base fluid which is chosen as water are in thermal equilibrium and no slip occurs between them.

The thermophysical properties of the base fluid and the solid particles are given in Table 1 (Oztop and Abu-Nada [26]). The thermophysical properties of the nanofluid are assumed to be constant except for the density variation in the buoyancy force term which is determined by the Boussinesq approximation. The fluid rises in the channel driven by buoyancy forces. The flow is assumed to be steady, unidirectional and fully developed. Under these assumptions, the equations governing the convective flow and heat transfer are:

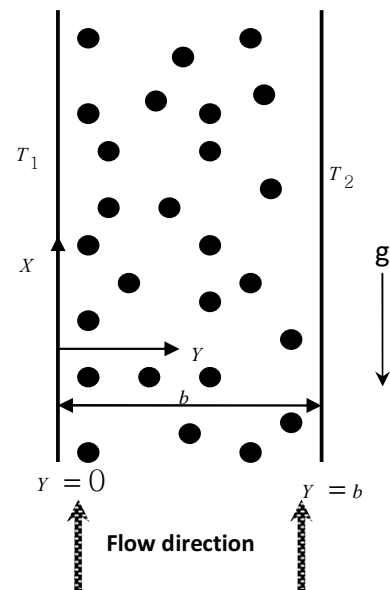


Figure 1. Physical configuration.

$$\mu_{nf} \frac{d^2 U}{dY^2} + (\rho\beta)_{nf} g (T - T_0) = 0 \quad (1)$$

$$\frac{d^2 T}{dY^2} + \left(\frac{\mu}{K}\right)_{nf} \left(\frac{dU}{dY}\right)^2 = 0 \quad (2)$$

along with boundary conditions

$$U = 0 \text{ at } Y = 0, b$$

$$T = T_1 \text{ at } Y = 0, T = T_2 \text{ at } Y = b \quad (3)$$

where U is the velocity component along Y -axis, g is the acceleration due to gravity, T is the temperature of the fluid, μ is the viscosity and K is the thermal conductivity of the fluid. The effective density of the nanofluid is given as

$$(\rho)_{nf} = (1-\phi)\rho_f + \phi\rho_s, \quad (4)$$

where ϕ is the solid volume fraction of nanoparticles. The thermal expansion coefficient of the nanofluid can be determined by

$$(\rho\beta)_{nf} = (1-\phi)(\rho\beta)_f + \phi(\rho\beta)_s. \quad (5)$$

The effective dynamic viscosity of the nanofluid given by Brinkman [27] is

$$\mu_{nf} = \mu_f / (1-\phi)^{2.5} \quad (6)$$

In equation (2), K_{nf} is the thermal conductivity of the nanofluid: For spherical nanoparticles, according to Maxwell [28], this can be written as

$$K_{nf} = K_f \left(\frac{K_s + 2K_f - 2\phi(K_f - K_s)}{K_s + 2K_f + \phi(K_f - K_s)} \right). \quad (7)$$

Here the subscripts nf , f and s respectively are the thermo-physical properties of the nanofluids, base fluid and the nano-solid-particles. The equations (1) to (3) are made dimensionless using the following

$$x = \frac{X}{b}, y = \frac{Y}{b}, u = U \frac{\rho_f}{\mu_f} b, \quad \theta = \frac{T - T_0}{T_2 - T_1},$$

$$T_0 = \frac{T_1 + T_2}{2}, \quad Gr = \frac{g \beta_f \Delta T b^3 \rho_f^2}{\mu_f^2},$$

$$Br = \frac{\mu_f^3}{K_f \Delta T \rho_f^2 b^2} \quad (8)$$

Equations (1) and (2) become

$$\frac{d^2 u}{dy^2} + A Gr \theta = 0 \quad (9)$$

$$\frac{d^2 \theta}{dy^2} + C Br \left(\frac{du}{dy} \right)^2 = 0 \quad (10)$$

and related boundary conditions (3) become

$$u = 0 \text{ at } y = 0, 1$$

$$\theta = -\frac{1}{2} \text{ at } y = 0, \theta = \frac{1}{2} \text{ at } y = 1 \quad (11)$$

$$\text{where } A = (1-\phi)^{2.5} \left(1 - \phi + \phi \frac{(\rho\beta)_s}{(\rho\beta)_f} \right),$$

$$C = \frac{1}{(1-\phi)^{2.5}} \left(\frac{K_s + 2K_f + \phi(K_f - K_s)}{K_s + 2K_f - 2\phi(K_f - K_s)} \right)$$

We shall solve this coupled nonlinear differential equation using the DTM, and compared the results numerically by finite difference method and the perturbation method. Such solutions are useful and serve as a baseline for comparison with the solutions obtained via numerical schemes.

Basic Idea of Differential Transformation Method (DTM)

The differential transform of function $u(y)$ is defined as

$$U(k) = \frac{1}{k!} \left[\frac{d^k u(y)}{dy^k} \right]_{y=0} \quad (12)$$

where $u(y)$ is the original function and $U(k)$ is the transformed function which is called the T-function. The differential inverse transform of $U(k)$ is defined as follows:

$$u(y) = \sum_{k=0}^{\infty} U(k) y^k \quad (13)$$

In real applications, the function $u(y)$ be a finite series, (13) can be written as

$$u(y) = \sum_{k=0}^n U(k) y^k \quad (14)$$

and (13) implies that $\sum_{k=n+1}^{\infty} U(k) y^k$ is neglected as it is small. Usually, the values of n are decided by a convergence of the series coefficients. In order to assess the accuracy of DTM for solving nonlinear equations the solutions obtained from DTM are compared with numerical solutions (FDM) and with analytical solutions (PM). The fundamental mathematical operations performed by differential transform method are listed in Table 2. Taking differential transform of Eqs. (9) and (10), one can obtain

$$U[k] = -\frac{A Gr}{(1+k)(2+k)} \Theta[k] \quad (15)$$

$$\Theta[k] = -\frac{C Br}{(1+k)(2+k)} \sum_{r=0}^k (k+1-r)(r+1) U[k+1-r] U[r+1] \quad (16)$$

The differential transform of the boundary conditions are as follows

$$U[0] = 0, U[1] = \alpha, \Theta[0] = -\frac{1}{2}, \Theta[1] = \beta \quad (17)$$

Using the conditions as given in Eq. (11), one can evaluate the unknowns α and β . By using the DTM and the transformed boundary conditions, above equations that finally leads to the solution of a system of algebraic equations.

Finite Difference Method (FDM)

The governing Eqs. (9) and (10) together with the boundary conditions (11) are solved using finite difference method. In numerical iterations, computational domain is divided into a uniform grid system. Both the second-derivative and the squared first-derivative terms are discretized with central difference of second-order accuracy and the results are presented in Tables.

Perturbation Method (PM)

Equations (9) and (10) are coupled non-linear equations because of viscous dissipations and it is difficult, in general, to solve them analytically. However for vanishing Br , equations become linear and can be solved exactly. Small values of Br facilitate finding analytical solutions of Eqs. (9) and (10) in the form:

$$u = u_0 + Br u_1 + Br^2 u_2 \dots \quad (18)$$

$$\theta = \theta_0 + Br \theta_1 + Br^2 \theta_2 \dots \quad (19)$$

Substituting (18) and (19) into (9) and (10) and equating the like powers of Br to zero, we obtain zeroth and first order equations. Zeroth order equations take the form

$$\frac{d^2 u_0}{dy^2} + A Gr \theta_0 = 0 \quad (20)$$

$$\frac{d^2 \theta_0}{dy^2} = 0 \quad (21)$$

subject to boundary conditions

$$u_0 = 0 \text{ at } y = 0, 1;$$

$$\theta_0 = -\frac{1}{2} \text{ at } y = 0; \theta_0 = \frac{1}{2} \text{ at } y = 1 \quad (22)$$

First order equations

$$\frac{d^2 u_1}{dy^2} + A Gr \theta_1 = 0 \quad (23)$$

$$\frac{d^2 \theta_1}{dy^2} + C \left(\frac{du_0}{dy} \right)^2 = 0 \quad (24)$$

subject to boundary conditions

$$u_1 = \theta_1 = 0 \quad \text{at} \quad y = 0, 1 \quad (25)$$

Solutions of Eqs. (20) and (21) using (22) are

$$\theta_0 = y - 0.5;$$

$$u_0 = \frac{-A Gr (1 - 3y + 2y^2)y}{12} \quad (26)$$

Solutions of Eqs. (23) and (24) are not presented due to brevity. The physical quantity of interest in this problem is the skin friction and Nusselt number which for the heated wall and cold wall. The dimensionless form of skin friction coefficient is

$$\tau_0 = \frac{1}{(1-\phi)^{2.5}} \frac{du}{dy} \Big|_{y=0} \quad \text{and} \quad \tau_1 = \frac{1}{(1-\phi)^{2.5}} \frac{du}{dy} \Big|_{y=1}$$

and the dimensionless form of Nusselt number is

$$Nu_0 = \left(\frac{K_{nf}}{K_f} \right) \frac{d\theta}{dy} \Big|_{y=0} \quad \text{and} \quad Nu_1 = \left(\frac{K_{nf}}{K_f} \right) \frac{d\theta}{dy} \Big|_{y=1}$$

III. Results and discussion

The problem of free convection in a vertical channel filled with nanofluid including the effects of viscous dissipation is analysed. The governing equations are highly nonlinear and coupled for which the closed form solutions are not available. However the approximate solutions are obtained using three different methods i.e. by DTM, FDM and PM. Error analysis is also done between these methods. In order to justify the results obtained by DTM, the problem is linearised and compared with DTM solutions. The solutions obtained by direct method and DTM agree very well. Further finding the solutions of nonlinear equations using FDM also justify the solutions obtained using DTM. To further justify the solutions of DTM, the nonlinear governing

equations are solved analytically using PM valid for small values of free convection parameter and Brinkman number.

The velocity and temperature fields are computed for various values of governing parameters such as Grashof number Gr (free convection parameter), solid volume fraction ϕ and Brinkman number Br for different nano-particles and are shown in Figs. 2 to 6. The values of all the graphs are obtained by DTM.

Figure 2 displays the velocity profiles for Ag, Cu, Diamond, TiO₂ and SiO₂ nano-particles. It is observed that the values for silver and copper show closer values and Diamond, SiO₂ and TiO₂ are also close to each other. The optimal velocity is observed using silver as a nano-particle at the hot wall and minimal value at the cold wall.

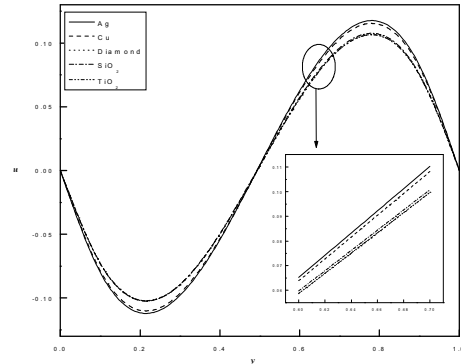


Fig. 2 Velocity profiles for different nanoparticles with $Gr = 20$, $\phi = 0.1$, $Br = 0.1$.

The flow field for different values of free convection parameter Gr and solid volume fraction ϕ is shown in Figs. 3 and 4 respectively. As Grashof number increases, velocity increases in the domain $y = 0.5$ to 1 decreases from $y = 0$ to 0.5. It is also observed from Fig. 3 that as the solid volume fraction ϕ increases velocity decreases. ($\phi = 0$ are the profiles for purely viscous fluid). As the Grashof number increases temperature increases slightly in the middle of the channel. Also as solid volume fraction ϕ increases temperature decreases. However the effects of Grashof number Gr and solid volume fraction ϕ on the temperature do not show significant effects on the temperature field.

Figures 5 and 6 are the plots of velocity and temperature for variations of Brinkman number Br and solid volume fraction ϕ . The nature of graphs is similar to the effect of Gr and ϕ as seen in Figs. 3 and 4 respectively. That is as Brinkman number increases velocity decreases near the cold wall and increases near the hot wall for both viscous and nanofluids. The effect of Br and ϕ on temperature is not very effective as seen in Fig. 6. The velocity and temperature profiles for viscous fluid are more when compared to nanofluid. This is due to the fact that adding nano-particles to viscous fluid will result in suspensions, similar to that of non-Newtonian fluids, hence adding additives to viscous fluid will result in the reduction of flow nature.

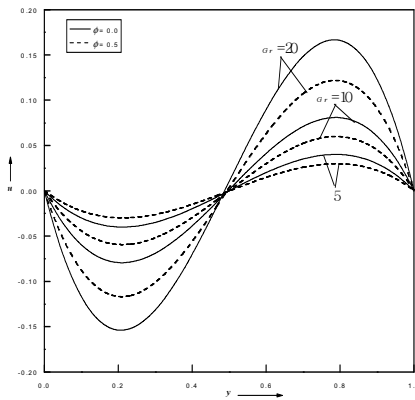


Fig. 3 Velocity profiles for different values of Gr and ϕ with $Br = 0.1$ for silver-water nanoparticles.

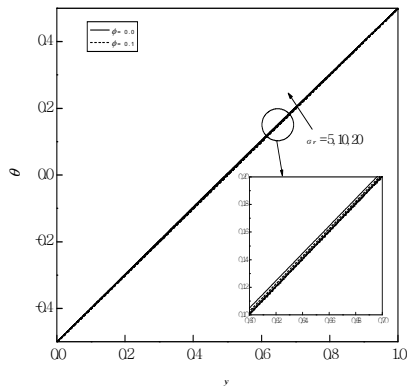


Fig. 4 Temperature profiles for different values of Gr and ϕ with $Br = 0.1$ for silver-water nanoparticles.

To understand the frictional force and rate of heat transfer, at the walls, plots of skin friction and Nusselt number are shown in Figs. 7 and 8 respectively. It is seen from Fig. 7 that skin friction at both the walls decreases as Grashof number increases. The Brinkman number increases the skin friction at the cold wall and decreases at the hot wall. However its effect is not significant for small values of Grashof number at both the walls. Figure 7 also shows that profiles of skin friction for nanofluid lies above viscous fluid at both the walls. The rate of heat transfer for variations of Grashof number, Brinkman number and solid volume fraction is shown in Fig. 8. The effect of Grashof number on heat is not very effective at both the walls. As Brinkman number increases skin friction at the cold wall increases and decreases at the hot wall for large values of Grashof number. The plots of heat transfer at both the walls for nanofluid lies below the viscous fluid.

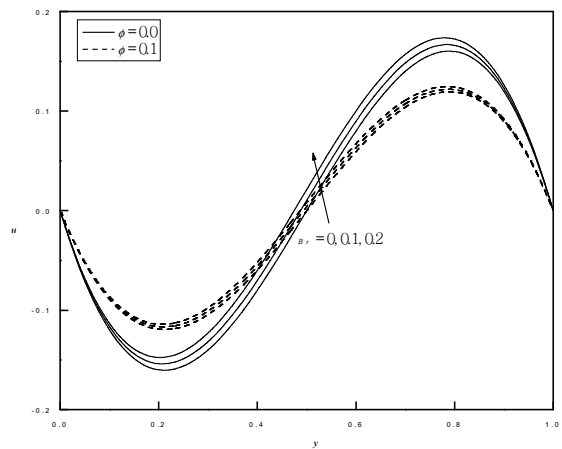


Fig. 5 Velocity profiles for different values of Br and ϕ with $Gr = 20$ for copper-water nanoparticles.

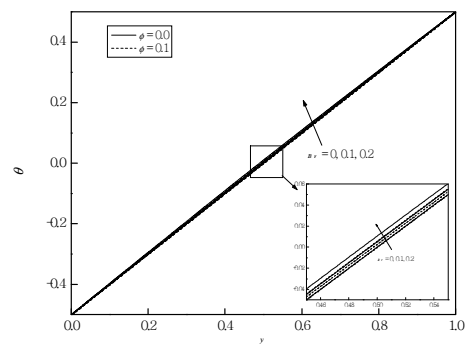


Fig. 6 Temperature profiles for different values of Br and ϕ with $Gr = 20$ for copper-water nanoparticles.

Table 3 and 4 shows the results obtained by DTM, FDM and PM. In the absence of viscous dissipation Eq. (9) to (10) reduces to linear ODEs. Table 3 shows the results of exact solution with the results of DTM solution is agree very well. Table 4 shows the results of temperature for different nano-particles. We observe that convection for SiO_2 is more then followed by Silver, Copper, TiO_2 and less for Diamond. In the presence of viscous dissipations the results are shown in Table 5. It is obvious that present method provides more acceptable results compare with FDM and PM even for $Br = 1$.

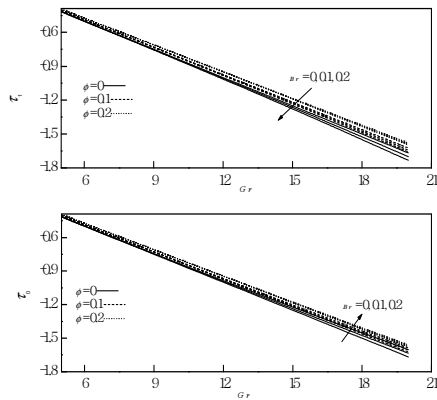


Fig. 7 skin friction profiles for different values of Gr , Br and ϕ for copper-water nanoparticles.

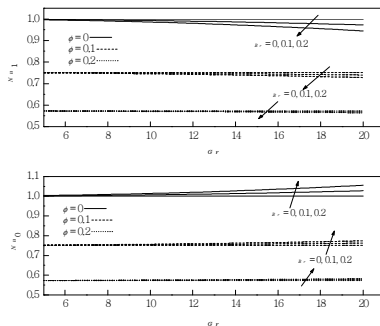


Fig. 8 Nusselt number profiles for different values of Gr , Br and ϕ for copper-water nanoparticles.

Table.1: Thermo-physical properties for pure water and various types of nanoparticles.

Property	Pure water	Ag	Cu	Diamond	SiO_2	TiO_2
ρ (kg/m ³)	997.1	10500	8933	3510	2200	4250
μ (Nm/s)	0.001	-	-	-	-	-
k (W/mK)	0.613	429	400	1000	1.2	8.9538
β (1/K) $\times 10^6$	207	18	17	1.0	5.5	0.17

Table 2: The operations for the one-dimensional differential transform method.

Original function	Transformed function
$y(x) = g(x) \pm h(x)$	$Y(k) = G(k) \pm H(k)$
$y(x) = \alpha g(x)$	$Y(k) = \alpha G(k)$
$y(x) = \frac{dg(x)}{dx}$	$Y(k) = (k+1)G(k+1)$
$y(x) = \frac{d^2g(x)}{dx^2}$	$Y(k) = (k+1)(k+2)G(k+2)$
$y(x) = g(x)h(x)$	$Y(k) = \sum_{l=0}^k G(l)H(k-l)$
$y(x) = x^m$	$Y(k) = \delta(k-m) = \begin{cases} 1, & \text{if } k = m \\ 0, & \text{if } k \neq m \end{cases}$

Table 3. Comparison of the values of velocity and temperature with exact solution in the absence of viscous dissipation $G_r = 10$ for copper-water nano-particles.

	Velocity				Temperature			
	$\phi = 0.0$		$\phi = 0.5$		$\phi = 0.0$		$\phi = 0.5$	
	Exact	DTM	Exact	DTM	Exact	DTM	Exact	DTM
0	0	0	0	0	-	-0.5	-0.5	-0.5
0.1	-0.06	-	-	-0.00920	-	-0.4	-0.4	-0.4
0.2	-0.08	-	-	-0.01227	-	-0.3	-0.3	-0.3
0.3	-0.07	-	-	-0.01073	-	-0.2	-0.2	-0.2
0.4	-0.04	-	-	-0.00613	-	-0.1	-0.1	-0.1
0.5	0	0	0	0	0	0	0	0
0.6	0.04	0.04	0.00613	0.00613	0.1	0.1	0.1	0.1
0.7	0.07	0.07	0.01073	0.01073	0.2	0.2	0.2	0.2
0.8	0.08	0.08	0.01227	0.01227	0.3	0.3	0.3	0.3
0.9	0.06	0.06	0.00920	0.00920	0.4	0.4	0.4	0.4
1	0	0	0	0	0.5	0.5	0.5	0.5

Table 4. Values of temperature field for different nano-metals in a channel with $Br = 0.1$ and $G_r = 20$.

y	Silver (Au)	Copper (Cu)	Diamond	SiO ₂	TiO ₂
0	-	-	-	-	-
0.1	0.500000	0.500000	0.500000	0.500000	0.500000
0.2	0.398965	0.399002	0.399143	0.398930	0.399102
0.3	0.298323	0.298383	0.298614	0.298265	0.298547
0.4	0.197718	0.197800	0.198114	0.197639	0.198024
0.5	0.097231	0.097331	0.097712	0.097135	0.097602
0.6	0.002956	0.002849	0.002442	0.003058	0.002560
0.7	0.102764	0.102665	0.102284	0.102859	0.102394
0.8	0.202281	0.202199	0.201885	0.202360	0.201975
0.9	0.301689	0.301628	0.301395	0.301748	0.301462
1	0.401057	0.401019	0.400872	0.401094	0.400914
1	0.500000	0.500000	0.500000	0.500000	0.500000

Table 5: Comparison of the values of velocity and temperature for copper-water nano-particles ($G_r = 10$, $\phi = 0.2$).

Br		Velocity			Temperature		
		DTM	FDM	PM	DTM	FDM	PM
0.5	0	0.00000000	0.00000000	0.00000000	0.50000000	0.50000000	-0.50000000
	0.1	-0.03220928	-0.03220867	-0.03220887	0.39932782	0.39932231	-0.39932679
	0.2	-0.04276671	-0.04276575	-0.04276594	0.29891368	0.29890962	-0.29891198
	0.3	-0.03711756	-0.03711645	-0.03711650	0.19852332	0.19852169	-0.19852123
	0.4	-0.02070450	-0.02070335	-0.02070328	0.09820857	0.09820755	-0.09820627
	0.5	0.00103412	0.00103527	0.00103540	0.00191299	0.00191515	0.00191536
	0.6	0.02267014	0.02267118	0.02267136	0.10178930	0.10179245	0.10179160
	0.7	0.03878819	0.03878898	0.03878925	0.20147616	0.20147831	0.20147825
	0.8	0.04398289	0.04398331	0.04398366	0.30109139	0.30109038	0.30109309
	0.9	0.03285301	0.03285313	0.03285342	0.40068135	0.40067769	0.40068239
1	0.00000000	0.00000000	0.00000000	0.50000000	0.50000000	0.50000000	
1.0	0	0.00000000	0.00000000	0.00000000	0.50000000	0.50000000	-0.50000000
	0.1	-0.03188789	-0.03188644	-0.03188706	0.39866414	0.39864463	-0.39866208
	0.2	-0.04215895	-0.04215697	-0.04215737	0.29783137	0.29781925	-0.29782796
	0.3	-0.03628207	-0.03628019	-0.03627992	0.19704489	0.19704338	-0.19704066
	0.4	-0.01972110	-0.01971943	-0.01971860	0.09641374	0.09641509	-0.09640907
	0.5	0.00206902	0.00207053	0.00207165	0.00382726	0.00383029	0.00383208
	0.6	0.02365388	0.02365510	0.02365639	0.10357774	0.10358491	0.10358244
	0.7	0.03962465	0.03962524	0.03962681	0.20295300	0.20295662	0.20295732
	0.8	0.04459227	0.04459210	0.04459387	0.30218890	0.30218075	0.30219245
	0.9	0.03317587	0.03317536	0.03317671	0.40137255	0.40135537	0.40137480
1	0.00000000	0.00000000	0.00000000	0.50000000	0.50000000	0.50000000	

IV. Conclusion

In this study, we presented the definition and operation of differential transformation method (DTM). The DTM has been utilized to derive approximate explicit analytical solutions for nonlinear free convection problem with a small parameter. This new method accelerated the convergence to the solutions. Moreover, it was shown that for this kind of problems, DTM is better than PM and FDM. The figures and tables clearly show this method provides excellent approximations to the solution of these nonlinear equations with high accuracy.

Acknowledgments:

The authors gratefully acknowledge the support of the UGC-New Delhi for funding the current research grant under UGC Major Research Project.

References

- [1] Ostrach, S. Natural convection in enclosures, *J. Heat Transfer*, 110, pp. 1175–1190, 1988.
- [2] S. Choi, Enhancing thermal conductivity of fluids with nanoparticle. in: D.A. Siginer, H.P. Wang (Eds.), *Developments and Applications of Non-Newtonian Flows*, MD vol. 231 and FED, 66. ASME, pp. 99-105, 1995.
- [3] H. Masuda, A. Ebata, K. Teramae, N. Hishinuma, Alteration of thermal conductivity and viscosity of liquid by dispersing ultra-fine particles, *Netsu Bussei*, 7, 227-233, 1993.
- [4] J. Buongiorno, W. Hu, Nanofluid coolants for advanced nuclear power plants, in: *Proceedings of ICAPP'05*, Seoul, Paper no. 5705 (May 15-19, 2005).
- [5] J.A. Eastman, S.U.S. Choi, S. Li, W. Yu, L.J. Thompson, Anomalous increased effective thermal conductivities of ethylene glycol-based nanofluids containing copper nanoparticles, *Appl. Phys. Lett.*, 78, pp. 718–720, 2001.
- [6] H.Q. Xie, H. Lee, W. Youn, M. Choi, Nanofluids containing multiwalled carbon nanotubes and their enhanced thermal conductivities, *J. Appl. Phys.*, 94,8, pp. 4967–4971, 2003.
- [7] S. Jana, A. Salehi-Khojin, W.H. Zhong, Enhancement of fluid thermal conductivity by the addition of single and hybrid nano-additives, *Thermo chimica Acta*, 462, pp. 45–55, 2007.
- [8] R-Y. Jou, S-C. Tzerg, Numerical research on natural convective heat transfer enhancement filled with nanofluids in rectangular enclosures, *Int. Commu. Heat Mass Transfer*, 33, pp. 727-736, 2006.
- [9] K. Khanafer, K. Vafai, M. Lightstone, Buoyancy-driven heat transfer enhancement in a two-dimensional enclosure utilizing nanofluids, *Int. J. Heat Mass Transfer*, 46, pp. 3639-3653, 2003.
- [10] W. Daungthongsuk, S. Wongwises, A critical review of convective heat transfer nanofluids, *Renew Sust Energy Rev*, 11, pp. 797–817, 2007.
- [11] V. Trisaksri, S. Wongwises, Critical review of heat transfer characteristics of nanofluids, *Renew Sust Energy Rev*, 11, pp. 512–523, 2007.
- [12] X. Wang, A.S. Mujumdar, Heat transfer characteristics of nanofluids: A review. *Int. J. Therm. Sciences*, 46, pp. 1–19, 2007.
- [13] Kumar, S., Prasad, S.K., Banerjee, J. Analysis of flow and thermal field in nanofluid using a single phase thermal dispersion model. *Applied Mathematical Modelling*, 34, pp. 573-592, 2010.
- [14] Dalia Sabina Cimpean, Ioan Pop, Fully developed mixed convection flow of a nanofluid through an inclined channel filled with a porous medium *Int. J. Heat and Mass Transfer*, 55, pp.907–914, 2012
- [15] J.K. Zhou, *Differential transformation and its applications for electrical circuits*. Huarjung University Press; 1986. (in Chinese)
- [16] M.J. Jang, C.L. Chen, Y.C. Liu, Two-dimensional differential transform for partial differential equations, *Appl. Math. Comput*, 121, pp. 261–270, 2001.
- [17] Kurnaz A, Oturanç G. The differential transform approximation for the system of ordinary differential equations. *Int J Comput Math*, 82, pp.709–19, 2005.
- [18] Arikoglu A, Ozkol I. Solution of differential-difference equations by using differential transform method. *Appl Math Comput*, 181, pp.153–62, 2006.
- [19] A.S.V. Ravi Kanth and K. Aruna, Solution of singular two-point boundary value problems using differential transformation method. *Physics Letters A*, 372, pp. 4671–4673, 2008.
- [20] M.M. Rashidi, The modified differential transform method for solving MHD boundary-layer equations. *Computer Physics Communications*, 180, pp. 2210–2217, 2009.
- [21] A.S.V. Ravi Kanth, K. Aruna, Differential transform method for solving the linear and nonlinear Klein–Gordon equation, *Computer Physics Commun*, 180, pp.708–711, 2009.
- [22] M.J. Jang, Y.L. Yeh, C.L. Chen, W.C. Yeh, Differential transformation approach to thermal conductive problems with discontinuous

- boundary condition. *Appl. Mathematics and Computation*, 216, pp. 2339–2350, 2010.
- [23] M.M. Rashidi, N. Laraqi, S.M. Sadri, A novel analytical solution of mixed convection about an inclined flat plate embedded in a porous medium using the DTM-Padé, *Int. J. Thermal Sciences*, 49, pp. 2405–2412, 2010.
- [24] Hessameddin Yaghoobi, Mohsen Torabi, The application of differential transformation method to nonlinear equations arising in heat transfer. *Int. Commu. Heat and Mass Transfer*, 38, pp. 815–820, 2011.
- [25] M. M. Rashidi, O. Anwar Beg, N. Rahimzadeh, A generalized differential transform method for combined free and forced convection flow about inclined surfaces in porous media, *Chem. Eng. Comm.*, 199, pp. 257–282, 2012
- [26] Abu-Nada, E. Application of nanofluids for heat transfer enhancement of separated flows encountered in a backward facing step. *Int. J. Heat and Fluid Flow*, 29, pp. 242-249, 2008.
- [27] H.C. Brinkman, The viscosity of concentrated suspensions and solution, *J. Chem. Phys.* 20, pp. 571-581, 1952.
- [28] J. Maxwell, A treatise on electricity and magnetism, 2nd ed. Oxford University Press, Cambridge, UK, 1904.

An Experimental Study of Effect of Welding Parameters on T- Weld Joint in TIG Welding of SS 316L and Development of its Microstructure and Mechanical properties

Rupinderpreet Singh^{#1}, Geetesh Goga², Lakhwinder Singh¹³

^{1,2,3}K.C.College of Engineering and I.T., Nawanshahr, Punjab, India

#rupi86_07@yahoo.co.in,*geeteshgoga@gmail.com,lerlakhwinders1@gmail.com

Abstract- The microstructure and tensile strength of T weld joint of stainless steel 316 material in TIG (tungsten inert gas) equipment was analysed by varying shielding gas (argon gas and Carbon dioxide) and voltage. Vastly different microstructures are formed in 316L stainless steel joints welded with Argon and Carbon dioxide and by varying voltage, respectively. Different microstructures, yield strength, tensile strength and weld bead hardness are tested in my project. Effect of varying voltage and shielding gas on stainless steel 316 material T-weld joint are analysed.

Keywords- TIG Welding, Argon, CO2, Operating Variables, Microstructures

I. INTRODUCTION

In the TIG (tungsten inert gas) welding process, an essentially non-consumable tungsten electrode is used to provide an electric arc for welding. A sheath of inert gas surrounds the electrode, the arc, and the area to be welded [1, 2, 6, 11]. This gas shielding process prevents any oxidization of the weld and allows for the production of neat, clean welds. TIG welding differs from MIG (metal inert gas) welding in that the electrode is not consumed in the weld. In the MIG welding process the electrode is continuously melted and is added into the weld. In TIG welding, no metal is added unless a separate filler rod is used. TIG welding can be performed with a large variety of metals. The two most commonly TIG welded metals in the PRL are steel and aluminium. Steel is relatively easy to TIG weld and it is possible to produce very tight, neat welds. Aluminium takes a little more skill, and one should have at least a little bit of experience in welding steel before making the transition to aluminium [4, 5, 8]. However, the basic technique is essentially the same and most people can make the jump to aluminium fairly easily. TIG welding is

an extremely powerful tool. With a little practice, it is possible to make beautiful welds much more quickly and

easily than with oxy-acetylene welding. It is also the only option currently available in the shop for welding aluminium. Put in a little time and you will be rewarded in spade. The shielding gas used in TIG welding can be argon, helium or a mixture of the two. Although the shop keeps a tank of the each next to the welding machine, the helium is almost never used except for special applications. Argon is usually a better choice because it is heavier than air and therefore tends to provide a better blanket over the weld [3, 9]. The flow from the argon tank is controlled by the regulator/flow meter which is screwed onto the top of the tank. The double seating main valve controls whether the argon will flow at all and the smaller valve at the bottom of the flow meter allows one to adjust the flow rate. Select a flow rate from this document's Appendix or from the guidelines posted on the TIG machine.

II. OPERATION

Following operating parameters were used during the operation

A. Operating Variables

Following are the operating variable in TIG

- Welding Current
 - Arc Voltage
 - Travel Speed
 - Size of Electrode
 - Electrode stick-out
 - Heat input rate
- ### B. Welding current

It controls the melting rate of the electrode and thereby the weld deposition rate. It also controls the depth of penetration. Too high a current causes excessive weld

reinforcement which is wasteful, and burn through in the case of thinner plates or in badly fitted joints, which are not proper backing. Excessive current also produces too narrow bead and under cut, excessively low current gives an unstable arc and over lapping. TIG control panel is usually provided with an ammeter to monitor and control the welding current.

C. Arc voltage

Arc voltage means the electrical potential difference between the electrode wire tip and the surface of molten weld pool. It is indicated by the voltmeter provided on the control panel. It hardly affects the electrode melting rate, but it determines the profile and surface appearance of the weld bead. As the arc voltage increases, the bead becomes wider and flatter, and the penetration decreases.

The bead width increases with an increase in arc voltage because an increase in arc voltage provides a longer arc which owing to its divergence is spread over a larger surface area thereby spreading the deposited metal over a wider area. The penetration as well dilution have been found to increase abruptly with the increase of arc voltage, but their rate of increase are found to be reduced significantly with further increase of arc voltage.

D. Travel speed

For a given combination of welding current and voltage, increase in welding speed result in lesser penetration, lesser weld reinforcement and lower heat input rate.

Excessively high travel speed decreases fusion between the weld deposit and the parent metal. Increases tendencies for under cut, arc blow, porosity and irregular bead shape. As the speed decreased, penetration and reinforcement increased. But too slow a speed result in poor penetration. Excessively high welding speed decreases the welding action and increases the probability of under cutting, causes blow weld porosity and uneven bead shapes. Excessively low speed also produces a convex hat shape beads that are subjects to cracking, cause excessively melt through, and produces a large weld puddle that flows around the arc resulting in rough bead, spatter and slag inclusions.

E. Size of electrode

At a given welding current, larger electrode results in wider, less penetration bead. Hence in joints with poor fit-up, a large electrode is preferred to a smaller one for bridging the root gap. For a given electrode size, a high current density results in a strong, penetration arc, while a lower current density gives a soft arc which is less penetrating.

F. Electrode stick-out

It is also termed as electrode extension. It refers to the length of the electrode, between end of contact tube and the arc, which is subjected to resistance heating at the high current densities used in the process. The longer the stick-out, greater will be amount of heating and higher the deposition. However, with the long stick-out, the increase in deposition rate is accompanied by a decrease rat in penetration. Hence longer stick-out is avoided when deep penetration is desired.

G. Heat input rate

Also termed arc energy, it is calculated by using formula as given below

$$HIR = (V \times A \times 60) / (S \times 1000)$$

Where HIR=Heat Input Rate (KJ/mm)

V= Arc Voltage

A = Welding Current (amp.)

S = Arc travel speed in mm/min.

For a given joint thickness, higher the heat input rate the lower is the cooling rate of the weld metal and (HAZ) heat affected zone of the parent metal, and vice versa. Heat input rate has an important bearing on the weld metal micro structure and the final structure of HAZ, and thereby on their toughness. The process usually is not suitable for use on metal less than 3/16 inch thick, because burn through is likely.

III. EXPERIMENTATION

A. Welding Equipments

For this purpose submerged arc welding equipment which is available to us is as follows:

- Fully automatic
- Circuit Voltage range 25-55 V
- Maximum Current 800 A
- Argon and Carbon Dioxide Gases are used as shielding gas.
- Electrode wire is of Stainless Steel single wire of diameter 3.16 mm.
- Stainless Steel 316L material is used for experimentation work.

B. Steps followed during the process

Tube of type AISI 316 with 100-mm length, 50mm diameter, 3mm thickness has been opted with welding voltage of 24, 40 and 55 Volts, and electrode type AWS E 316L. Electrode diameter was taken as nominal 2 mm with positive electrode Polarity and flat position. Pipe joint with 90degree angle and Root gap of 2 mm was kept. The two pieces to be welded were rigidly fixed with bolts at the edges in a fixture before welding process to

reduce the wrapping of the welded joint after welding. Then Tungsten Inert Gas Welding by varying voltage and shielding gas (Argon & CO₂) was done. Checking was also done for Microstructure on SEM Microscope, yield strength, tensile strength and hardness of weld bead. Experimental results are shown in diagrams and tables.

C. Gas Cutting

The oxy fuel process is the most widely applied industrial thermal cutting process because it can cut thicknesses from 0.5mm to 250mm.

D. Grinding and U-groove making

The U-groove is made with the help of cylindrical grinder in which one piece is grooved. Grinding is used to remove light rust and dirt also.

E. Rooting

The separation of the members to be welded together at the root to avoid the leakage of fused metal.

F. Welding with the help of TIG machine

After the rooting process for each specimen is over welding with the help of TIG machine at different parameters is made. After this welding by TIG process, the samples for testing the Yield Stress,



Figure 1. Welding with TIG Machine

Ultimate Tensile test are made, microstructure test are conducted of which the results are attached with.

IV. TEST REPORTS

Following are the test reports for the experimentation

A. Materials

AISI-316L austenitic stainless steel samples consisting of metal pipes of size 100x50x3 mm were welded using three two inert gases by varying voltage: Argon gas and

CO₂ gas . Austenitic AISI 316L stainless steel has an fcc structure. It has good weld ability due to its low carbon content, what makes it more difficult for chrome carbides to form on grain boundaries when welding. This steel is used extensively in the chemical and petro chemical industry. Austenitic AISI-308L stainless steel is widely used, especially in manufacturing equipment for corrosive food products. It gives excellent results when applied as welding rods in welding.

Table I
Chemical composition of the used plate and electrode E316L

Material	Tube (wt%)	Electrode (wt%)
C	0.075	0.02
Cr	17.4	18.5
Ni	11.0	12.0
Si	05.0	0.7
P	0.04	-
S	0.009	-
Mo	2.3	2.6
Mn	1.6	0.8
Fe	Bal	Bal

B. Microstructure Test

All samples, after each TIG welding with Argon gas and Co₂ gas as shielding gas with varying voltages were ground and polished using standard metallographic techniques and were subsequently etched in a marble etchant, which has chemical compositions as follows; 10 g. CuSO₄, 50 ml HCl and 50 ml H₂O. The microstructures of reheat-treated samples were viewed using scanning electron microscope (SEM) in the secondary electron mode. The size and area fraction of gamma prime particles were determined by the image analysis software.

C. Hardness Test

Vickers micro-hardness Tester is a key piece of equipment that is indispensable to metallographic research, product quality control, and the development of product certification materials. Vickers micro hardness test procedure as per ASTM E-384, EN ISO 6507, and ASTM E-92 standard specifies making indentation with a range of loads using a diamond indenter which is then measured and converted to a hardness value This machine used to make at least ten hardness indentations on the studied weld deposit specimens in the as weld and after heat treatment conditions. The Also, the test was carried out for the weld joint at the base metal; heat affected and welds metal zones. The applied load is 300 mg and the indentation time is 30 according to ASTM E92-72. The arithmetic mean, the

maximum and minimum values of the hardness number of each specimen are determined.

D. Micro structures

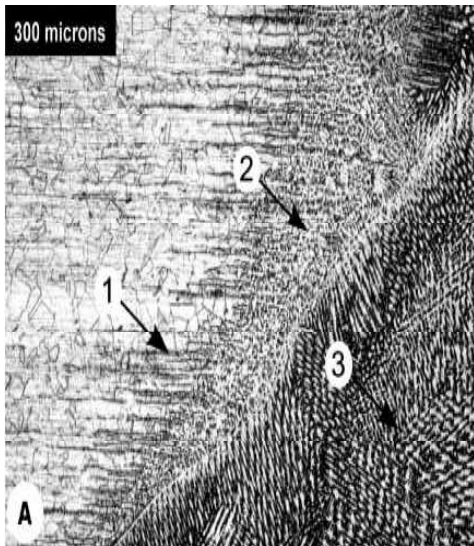


Figure 2 Micrographs of the AISI-316L steel welds with CO₂ gas as shielding gas at 40 volts.

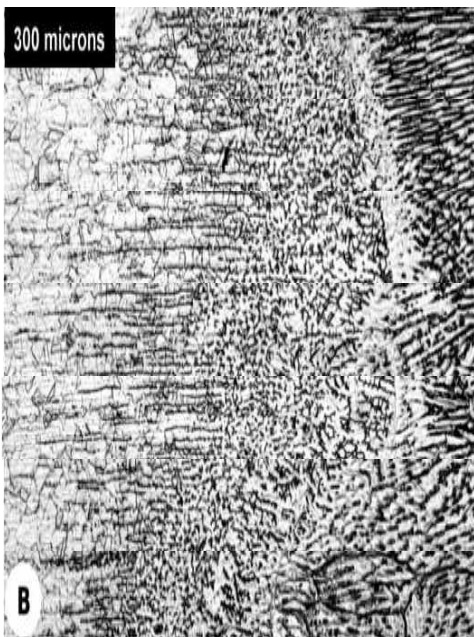


Figure 3 Micrographs of the AISI-316L steel welds with Argon gas as shielding gas at 40 volts.

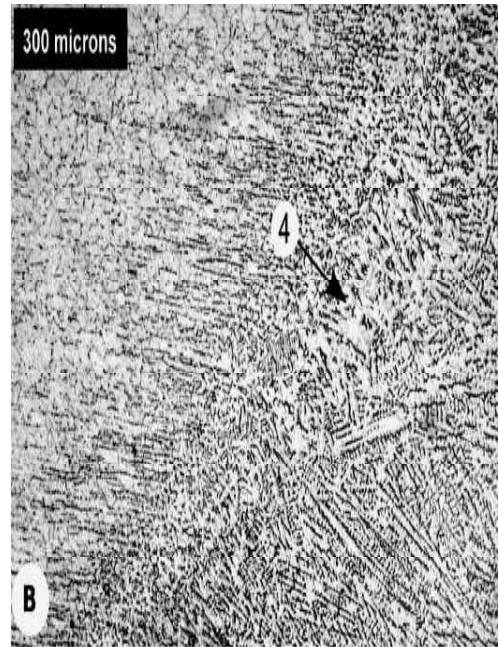


Figure 4 Micrographs of the AISI-316L steel welds with Argon gas as shielding gas with 55 volts voltage in room conditions

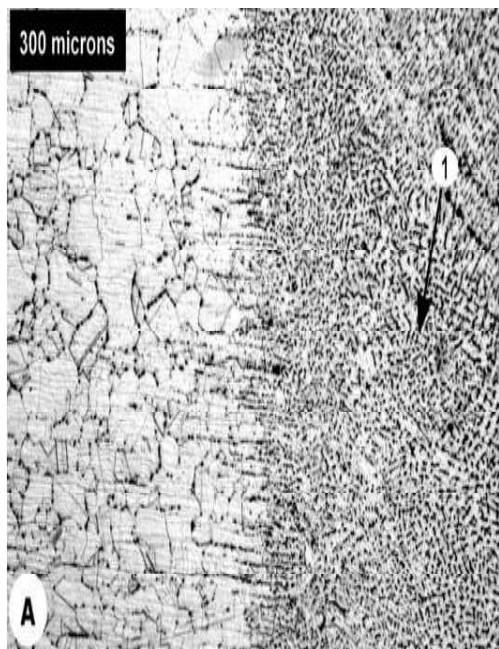


Figure 5 Micrographs of the AISI-316L steel welds with CO₂ gas as shielding gas with 55 volts.

E. Metallographic Structure

Figure 2 & 3 shows the microstructure of the zone of transition from the bed to the base metal when using Co₂ gas as shielding gas in room conditions at 55 volts (Figure 2) and when the inert gas Argon was used with 55 volts (Figure 3). An equiaxed austenitic structure typical of stainless steel can be observed on the left-hand side of each image. It is smaller than that of the base material, due to the changes that appear at the HAZ (heat affected zone). At the near fusion boundary, the structure presents smaller equiaxed grains of austenite (Figure 4) with ferrite stringers. The morphology of the weld bed shows duplex structure of austenite plus skeletal ferrite (Figure 5), although near the base metal the ferrite becomes interdendritic (Figure 6). The use of the Argon gas as shielding gas increased notably the size of the transition zone between the bed and the base metal. This is why figure 6 presents a wider area of both interdendritic ferrite and ferrite stringers. Also, finely distributed chrome carbide precipitates were detected when the weld was performed with CO₂ gas, but not when the inert gas Argon was used. Figure 4 & 6 corresponds to the welds carried out with AISI 308L using the usual TIG procedure with CO₂ gas as shielding gas (A) and the Argon as shielding gas (B). A completely austenitic structure can be observed in the base material for the HAZ, with a notable reduction in grain size for the samples that were welded using the Argon gas as shielding gas. At the bed, the use of the Argon gas shielding gas induced a change from interdendritic (1 in Figure 5) to skeletal ferrite (2 in Figure 6), with zones of lathy ferrite (3 in Figure 6), signal of a faster cooling due to the continuous argon supply. The micrographs (Figure 7) of the AISI 316L steel welded with Argon gas as shielding gas and CO₂ gas shielding gas shows the same structures than the other two: a reduction of austenitic grain size at the HAZ, ferrite stringers (1 in Figure 7) at the near fusion boundary and a zone of interdendritic ferrite (2 in Figure 7) at the beginning of the bed. Because of the great differences in composition between Argon and CO₂, the weld bed, which presents a full austenitic columnar solidification (3 in Figure 7), is separated from the partially melted zone by a clearly marked line.

F. Mechanical Characteristics

As can be seen in tables I and III, the micro structural changes that appear due to the presence of a weld bed - when the inert gas Argon is not used - increase the elastic limit of the material but reduce its tensile strength and its strain. Table III shows the tensile characteristics of the various joints according to the standardized tests

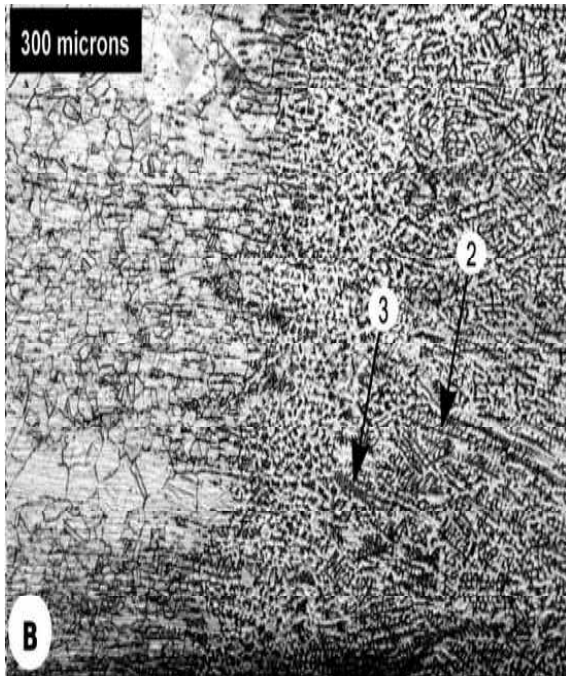


Figure 6 Micrographs of the AISI-316L steel welds with Argon gas as shielding gas with 25 volts voltage in room conditions

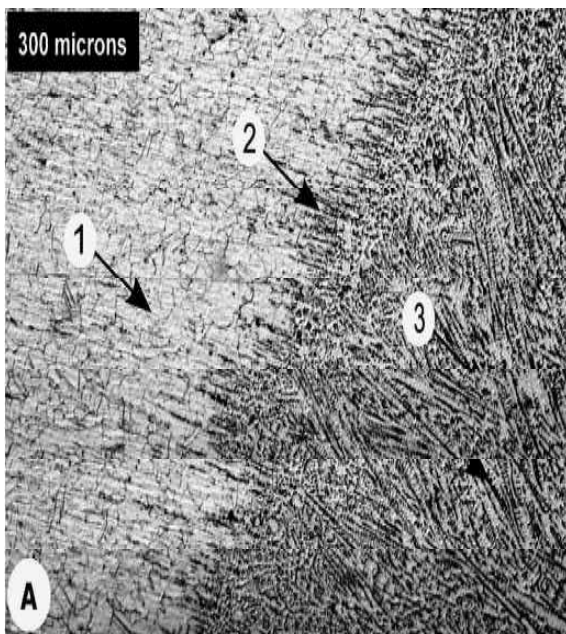


Figure 7 Micrographs of the AISI-316L steel welds with CO₂ gas as shielding gas with 55 volts.

specified in UNE–EN 895 and hardness in the bed, interface and heat affected zone (HAZ), as per Standard UNE 6507-01. As can be seen in tables I and III, the micro structural changes that appear due to the presence of a weld bed -when the inert gas Argon is not used- increase the elastic limit of the material but reduce its tensile strength

Table II
316L STEEL TIG WELD IN AMBIENT CONDITIONS WITH ARGON

Material	AISI 316L	AISI 316L	AISI 316L
Voltage in Volts	25	40	55
Yield strength MPa	318.5	325.0	345.5
Tensile strength MPa	410	450	495
Hardness (HV) base material	339	339	339
Hardness (HV) base material	328	335	348

Table III shows the tensile characteristics of the various joints according to the standardized tests specified in UNE–EN 895 and hardness in the bed, interface and heat affected zone (HAZ), as per Standard UNE 6507-01. As can be seen in tables I and III, the micro structural changes that appear due to the presence of a weld bed -when the inert gas Argon is not used- increase the elastic limit of the material but reduce its tensile strength and its strain.

Table III
316L STEEL TIG WELD IN AMBIENT CONDITIONS WITH CO2

Material	AISI 316L	AISI 316L	AISI 316L
Voltage in Volts	25	40	55
Yield strength MPa	315.5	322.5	330.0
Tensile strength MPa	402.5	425.0	468.5
Hardness (HV) base material	339	339	339
Hardness (HV) base material	298.5	318.5	330

At the same time, hardness at the weld increases notably if compared to the original alloy if the filler metals are the stainless steels but experiment no substantial changes if CO2 is used. These facts imply a slight deterioration of the mechanical characteristics of the welded structure due to fact that the weld is a linear zone of higher fragility. The use of an inert gas Argon and stainless steel pipes increases even more the yield strength despite the filler metal and reduces the tensile strength. On the other side, a much less increment in hardness is noted when welding with inert gas Argon, in fact the reduction in hardness ranges from a 28 % with 308L as using Argon as shielding gas at 55 volts to more than 50 % with Co2 gas as shielding gas at 55 volts. Although the decrease in tensile strength is not desirable, the lower hardness values obtained with the use of the inert Argon lead to assuring a non fragile behaviour of the joint, which can be useful. In this case, the yield strength reaches its higher value, but the tensile strength and hardness are also improved, obtaining values, for some parameters, almost identical to that of the base metal: values of harness around 154 HV were measured at the weld bed and the interface and a tensile strength only a 0.04 % lesser than the corresponding to the base metal. Although, due to limitations in size and economic requirements, its use is only advisable for demanding applications, hard-to-weld metals.

V. CONCLUSIONS

The use of an inert gas Argon as shielding gas resulted in a wider interface between the weld bed and the base metal, increasing both the presence of ferrite stringers and vermicular ferrite. Its use caused, in every case, a decrease of hardness and an increase of tensile strength and yield strength. On the other hand, the tensile strength was reduced, except when Argon gas is used as shielding gas at 55 volts. The weld carried out with Argon gas as shielding gas, presented the best characteristics. It combined high elongation and the best mechanical properties of all, very similar to that of the original 316L, which assures the best behaviour of the joint by maintaining the continuity of the mechanical characteristics in a welded structure.

REFERENCES

- [1] Anderson, P C J. The TIG welding of duplex and super duplex stainless steel. Seminar: The TIG Welding of Duplex Stainless Steel, Aberdeen, December 1993.
- [2] Baxter, C F G, Stevenson, A W and Warburton, G R. Welding of *zeron 100* duplex stainless steel. Proc conf

Intl Offshore and Polar Engineering, Singapore, June 1993.

[3] Gunn, R N. The weldability and properties of duplex and super duplex stainless steels. Proc conf Intl Offshore and Polar Engineering, Singapore, June 1993.

[4] Ogawa, T and Koseki, T. Effect of composition profiles on metallurgy and corrosion behaviour of duplex stainless steel weld metals. *Welding journal*,68(5), May 1989, 181s - 191s.

[5] Kokawa, H, Kuwana, T and Okada, J. Nitrogen absorption and microstructure of duplex stainless steel weld metal. *Welding International*, 7(5), 1993@384 -389.

[6] Anderson, P C J and Blunt, F J. An assessment of Ar-He-N₂ shielding gases for the TIG welding of duplex stainless steel. TWI members report 7251.01/93/781.1.

[7] Urmston, S and Creffield, G. Welding duplex stainless steels. Letter in *Welding & Metal Fabrication*, 61(9), November/December 1993, 451.

[8] Anderson, P C J and Gunn, R. Welding duplex stainless steels - further data. Letter in *Welding & Metal Fabrication*, 61(6), July 1993, 290.

[9] Bradshaw, R and Cottis, R A. Development and control of welding procedures for duplex stainless steels. *Welding & Metal Fabrication*, April 1993, 61(3)9 129 - 136.

[10] Beck Hansen, E. Emission of fume and gases in gas shielded arc welding. Intl Cutting and Welding Seminar, Essen, 1989, paper 3.

[11] Health and Safety Executive: Occupational exposure limits 1994. Document EH40/94.

[12] British Standard 6691, pt 2: Fume from welding and allied processes. BSI, 1986

©JITCE PUBLICATION